Ciencia y Tecnología, 31(1): 26-37, 2015
ISSN: 0378-0524

DIRECT FUNCTIONALIZATION OF Mn_{12}-(METHACRYLATE) CLUSTERS ON Si(100): SURFACE CHARACTERIZATION AND ELECTROCHEMICAL PROPERTIES

Marisol Ledezma-Gairaud,[1,2] Thomas Moehl[3], Mavis L. Montero[1,2] and Leslie W. Pineda,[1,2]

[1]*Centro de Electroquímica y Energía Química, CELEQ, Universidad de Costa Rica, San José, Costa Rica*
[2]*Escuela de Química, Universidad de Costa Rica, San José, Costa Rica*
[3]*Laboratory for Photonics and Interfaces, Institute of Chemical Sciences and Engineering, School of Basic Sciences, Ecole Polytechique Fédérale de Lausanne, CH-1015 Lausanne, Switzerland*

Received June 2015; accepted May 2015

Abstract

The reaction of H–terminated Si(100) with methacrylate–substituted manganese carboxylate clusters $[Mn_{12}O_{12}\{CH_2C(CH_3)COO\}_{16}(H_2O)_4]$, [$Mn_{12}$–(methacrylate)] via hydrosilylation afforded Mn_{12}–(methacrylate)–Si(100). The chemically modified surface was studied with an atomic force microscope (AFM), X–ray photoelectron spectra (XPS), a cyclic voltammeter (CV) and electrochemical impedance spectra (EIS). XPS show several Mn and Si electronic signatures that indicate the tailoring of Mn_{12}–(methacrylate) on the surface. The CV plot of Mn_{12}–(methacrylate)–Si(100) has two irreversible cathodic waves at –0.76 and –0.44 V, assigned to Mn(IV)/Mn(III) and Mn(III)/Mn(II) processes. The calculated charge at –0.44 V was 3.14 x 10^{-5} C cm^{-2}. An equivalent-circuit model was proposed based on EIS data and element circuit analysis. EIS show that the electronic and structural features of Mn_{12}–(methacrylate) on a surface greatly influence the electron transfer.

Resumen

La reacción de Si(100)–H con grupos carboxilato del clúster $[Mn_{12}O_{12}\{CH_2C(CH_3)COO\}_{16}(H_2O)_4]$, [$Mn_{12}$- (metacrilato)] a través de la química de hidrosililación, proporciona el Mn_{12}-(metacrilato)– Si(100). La superficie modificada químicamente se estudió mediante microscopía de fuerza atómica (AFM), espectroscopia de fotoelectrones de rayos X (XPS), voltametría cíclica (CV), y la espectroscopia de impedancia electroquímica (EIS). Los espectros XPS muestran características electrónicas del Mn y del Si que indican la incorporación del Mn_{12}-(metacrilato) en la superficie. El gráfico CV de Mn_{12}-(metacrilato)–Si (100) tiene dos ondas catódicas irreversibles en –0.76 y –0.44 V, que pueden ser asignadas a procesos redox Mn(IV)/ Mn(III) y Mn(III)/Mn(II). La carga calculada a –0,44 V es 3,14 x 10^{-5} C cm^{-2}. Un modelo de circuito equivalente se propuso con base en los datos de la EIS y el análisis de elementos del circuito. Las características electrónicas y estructurales del Mn_{12}-(metacrilato) en la superficie influyen en gran medida en la transferencia de electrones como se muestra por EIS.

Key words: Silicon(100), Mn_{12} cluster, cyclic voltammetry, X–ray photoelectron spectra (XPS), electrochemical impedance spectra (EIS).

Palabras clave: Silicio (100), complejo Mn_{12}, voltametría cíclica, Espectroscopía fotoelectrónica de Rayos-X (XPS), Espectroscopía de impedancia electroquímica (EIS).

* Corresponding author: leslie.pineda@ucr.ac.cr

I. INTRODUCTION

Modified surfaces of silicon are currently of great interest because several electronic components (e.g., rectifiers, junctions, switches, transistors, sensors etc.) rely on silicon semiconductor technology [1–6]. Related to these applications, various chemical protocols to attain novel surface properties have been reported, for instance, covalent functionalization under thermal conditions, electrochemical process, hydrosilylation catalysis, or photochemical reactions with alkenes, Grignard reagents or aldehydes [7–12]. In this vein, molecularly based devices integrating organic and inorganic hybrid interfaces might greatly enhance the properties and performance of semiconductors [13, 3]. Of particular interest are single–molecule magnets (SMM) that function as individual nanoscale magnetic particles; for instance, $[Mn_{12}O_{12}(O_2CR)_{16}(H_2O)_4]$ (R = Me, denoted as Mn_{12}–(OAc); Et, Ph) stores magnetic information based on a hysteresis cycle under cryogenic conditions [4,14]. This cluster is composed of a central $Mn_4(IV)O_4$ cubane and peripherical Mn(III) ions; the oxidation state of the latter is associated with a high–spin (d^4) electronic configuration that typically causes an elongation of manganese bonds known as a Jahn–Teller (JT) distortion (S1, Supplementary Information). Mn atoms in Mn_{12} clusters are active in oxidation and reduction, as demonstrated by electrochemical measurements in solution [14]. The integration of Mn_{12} clusters onto Si wafers has been accomplished mostly through a step-wise method requiring surface prefunctionalization with chemical groups that provide specific docking sites; the reports [12, 13] neglect any electrochemical characterization of the surface.

To study their integration as a source of novel electronic properties coupled to silicon, we reported the tailoring of copper(II) bimetallic complexes on Si(100) [16]; the electronic and structural features of the coordination complex led to the formation of multilayers using linking molecules to anchor additional molecules. The immobilized copper atoms are electroactive, showing well defined redox states. In the case of the Mn_{12} cluster, its coordination chemistry might also render prospective applications as units for information storage on a molecular scale, given the multiple stable discrete oxidation states in the molecule. In this work, we investigated the direct grafting of Mn_{12}–(methacrylate) onto a silicon surface rather than through a step-wise method requiring a ligand displacement to assemble Mn_{12}–(methacrylate)–Si(100). Such a surface array is substantially nearer the silicon substrate, and in theory would allow for a more robust and facile electron transfer. To this end, the elemental composition of the surface was characterized with an atomic-force microscope (AFM) and X–ray photoelectron spectra (XPS); the electrochemical properties and charge transfer at the interface of the electrolyte/Mn_{12}–(methacrylate)–Si(100) electrode/Si structure were investigated with a cyclic voltammeter (CV) and electrochemical impedance spectra (EIS) [17].

II. Experiments

General:

All chemical and solvents were used as received; all preparation and manipulations were performed under aerobic conditions, except as otherwise noted. The substrates were *n*–type Si(100) (Ultrasil Corporation, 0.001–0.002 ohm cm^{-1}). $[Mn_{12}O_{12}\{CH_2C(CH_3)COO\}_{16}(H_2O)_4]\cdot 4CH_2C(CH_3)COOH\cdot CH_2Cl_2$, ($Mn_{12}$–(methacrylate) was synthesized as described elsewhere [18].

H–terminated Si(100) surface preparation, (Si–H)

Si(100) wafers (1x1 cm^2) were cleaned in an ultrasonic bath using solvents toluene, acetone, isopropanol and water for 10 min each. The wafers were dried in a stream of flowing dinitrogen. Si(100) pieces were then oxidized at high frequency for 5 min (each wafer side) in a plasma cleaner (Harrick PDC–32G), followed by dipping in an aqueous solution of HF (1%) for 3 min, and dried in a stream of dinitrogen.

Mn_{12}–(methacrylate) clusters on Si(100), Mn_{12}–(methacrylate)–Si(100)

H–terminated Si(100) was soaked in a solution of Mn_{12}–(methacrylate) and benzoyl peroxide (BPO) in dichloromethane (CH_2Cl_2) (1.0 mmol L^{-1}) at 60 °C for 1 h under dinitrogen protection. The substrates were washed twice with CH_2Cl_2 in an ultrasonic bath for 10 min, and dried under flowing dinitrogen.

Surface characterization

An AFM (Veeco, Nanoscope IIId Digital Instruments, Santa Barbara, CA) was operated in the tapping mode; the images were analyzed using software (NanoScope). The root-mean-square (rms) result for each substrate was calculated for at least three samples and in three areas.

CV was performed with a potentiostat (Autolab PGSTAT10) and a conventional three–electrode system; all measurements were undertaken near 23 °C. The reference electrode was constructed on sealing a Ag/AgCl wire into a glass tube with a solution of KCl (3 mol L^{-1}). The CV of Mn_{12}–(methacrylate) clusters was measured at scan rate 0.100 V s^{-1}, in a solution of NBu_4ClO_4 in acetonitrile (0.25 mol L^{-1}). The CV of Mn_{12}–(methacrylate)–Si(100) were measured with a *n*–type Si(100) working electrode (1 cm x 1 cm) in an enclosed and grounded Faraday cage. A small area of the working electrode was wetted with the electrolyte to maintain a small overall area of measurement; this practice ensured that the RC time coefficient of the electrochemical cell was sufficiently small that rapid kinetic events were accurately measured. A bare silver wire served as the counter/reference electrode; this electrode was prepared on sonicating Ag wire in aqueous NH_3 (7.0 mol L^{-1}), rinsing it in deionized water and ethanol, and sonicating it in dichloromethane. The prepared wire was placed inside a polypropylene disposable pipet tip (10 μL) containing an electrolyte solution (KCl, 3 mol L^{-1}, ca. 5 μL). The working electrode was mounted on a Cu plate with a Ga–In eutectic to provide electrical contact through the back side of the wafer. A polypropylene micropipette tip, containing an Ag counter/reference electrode was filled with the electrolyte solution [19] (S2, Supplementary Information).

EIS were measured with a potentiostat/frequency analyzer (Autolab PGSTAT10). The AC voltage amplitude was 10 mV; the voltage frequencies used for EIS measurements ranged from 20 kHz to 0.100 Hz. The applied potential was –0.47 V vs. Ag/AgCl. Integration durations were set such that at least five cycles were analyzed at each point during each 1 s.

XPS were recorded (Thermo K–Alpha) with monochromated X–rays (12 kV, 6 mA), spot size 400 μm and takeoff angle 90° relative to the surface, with a typical duration 2–7 min in total of exposure per spot (typically three spots) to minimize beam damage. The binding energy was calibrated on centering the C 1s signal at 285 eV. Surveys were effected with pass energy 200 eV whereas high-resolution spectra were acquired with pass energy 50 eV. Typical pressures during analysis were less than 10^{-8} Torr.

III. RESULTS AND DISCUSSION

Our synthetic approach directly onto the silicon surface took advantage of functionalization with the dodecamanganese cluster via hydrosilylation chemistry. The reaction path occurs presumably through homolytic cleavage of benzoyl peroxide to form two benzoyloxy radicals, which further decompose to carbon dioxide and aryl radical [20, 21] (Figure 1). The latter species abstracts a hydrogen atom from Si–H groups resulting in silicon radicals on the surface that rapidly undergo nucleophilic addition through unsaturated bonds [11, 20, 21].

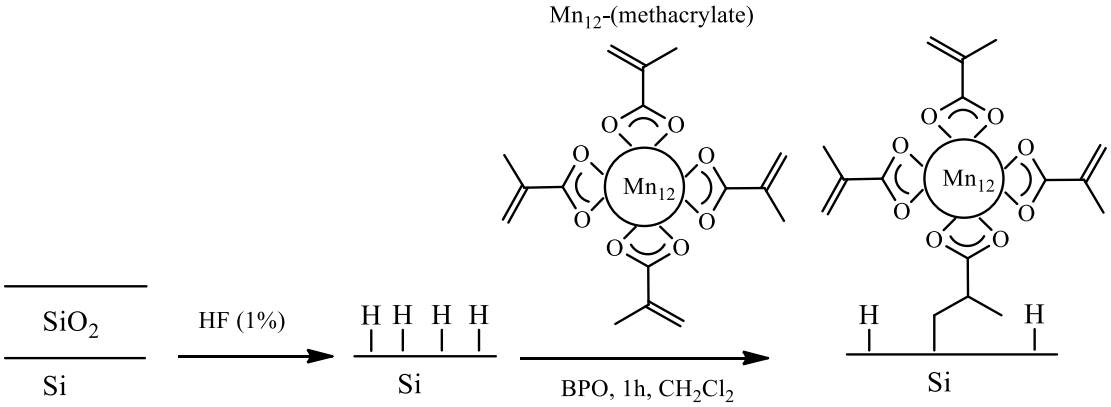

FIGURE 1. Reaction path for the preparation of Mn_{12}–(methacrylate)–Si(100).

AFM topographic characterization

Both roughness and topographic traits of Mn_{12}–(methacrylate)–Si(100) were measured with an AFM operated in tapping mode. The 3D profile of the surface shows several protruding features following functionalization with Mn_{12}–(methacrylate) (Figure 2), which differs from an AFM image of hydrogen–terminated silicon featuring a flat surface (S3, Supplementary Information).

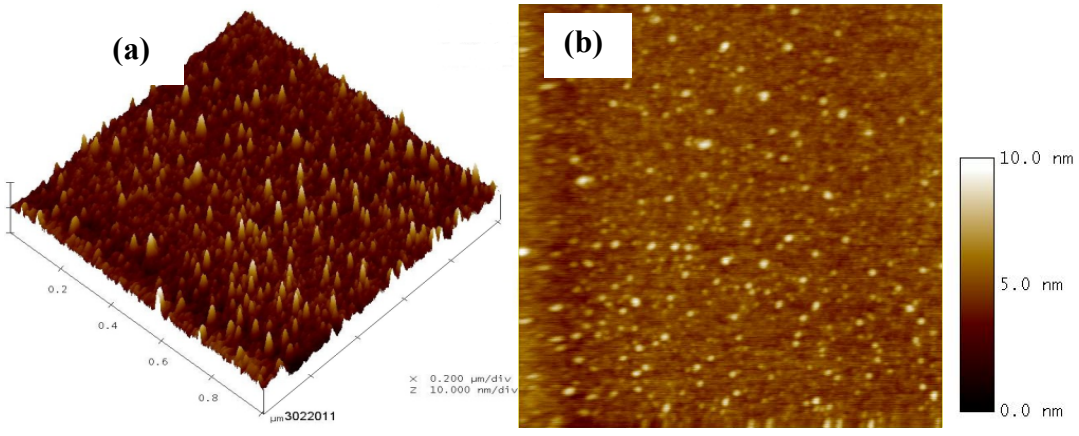

FIGURE 2. Tapping–mode AFM images of Mn_{12}–(methacrylate)–Si(100): (**a**) 3D image; (**b**) roughness.

The topography of Mn_{12}–(methacrylate)–Si(100) (average statistical roughness, R_a = 0.90 nm) indicates larger roughness than of a hydride-terminated Si surface (R_a = 0.30 nm), and

correlates well with the vertically maximal extension of carboxylate substituents bound in an axial position at Mn(III) ions, as shown by X–ray crystallographic data for Mn_{12}–(methacrylate): 1.04 nm, and Mn_{12}–OAc: 0.8 nm [21]. The root-mean-square roughness amplitude (1.28 nm) was greater than for a H–terminated Si surface (0.10 nm).

XPS results

Given that Mn(III) ions produce JT elongations, this effect can be thoroughly assessed with XPS analysis that allow assignment of binding energies [22, 23]. Table 1 summarizes the signals for the elements present on the functionalized surface from a XPS survey (S4, Supplementary Information).

TABLE 1. Binding energies obtained from X–ray photoelectron spectra of Mn_{12}–(methacrylate)–Si(100)

	assignment	**binding energy /eV**
Mn_{2p}	$2p_{½}$	653.9
	$2p_{3/2}$	642
C_{1s}	C–Si	285.2
	O–C=O	292.9
	CH_3, CH_2	286.9 and 288.7
O_{1s}	COO^-	532.5
	Mn–O	530
Si_{2p}	$2p_{3/2}$	99.7
	$2p_{½}$	100.4

The XPS of Mn_{12}–(methacrylate)–Si(100) has two lines at 653.9 and 642 eV, which are assigned to Mn 2p signals corresponding to excitation of $2p_{½}$ and $2p_{3/2}$, respectively. The main feature (experimental data) centred at 642 eV shows two components at 642.1 and 644.7 eV on deconvolution of the Mn 2p feature, ascribed to oxidation states Mn(III) and Mn(IV), respectively (Figure 3). The intensity ratio of Mn(III)/Mn(IV) signals is approximately 2, in accordance with the ratio Mn(III)/Mn(IV) for the molecular core.

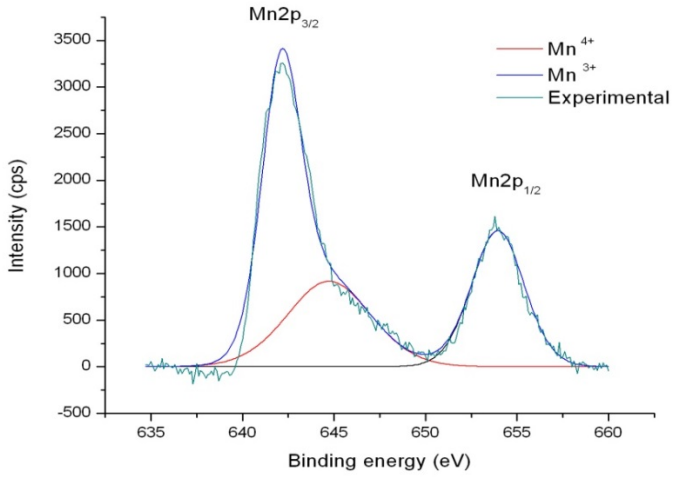

FIGURE 3. High-resolution XPS of the Mn 2p region in Mn_{12}–(methacrylate)–Si(100).

The Si 2p region is a reliable indicator of grafting on the surface. The XPS survey displays well resolved Si $2p_{3/2}$ / Si $2p_{½}$ spin-orbit doublets of elemental silicon (99.7 and 100.4 eV). A line at 103.3 eV is attributed to oxidized Si, likely due to some free Si–H bonds (umbrella effect on grafting bulky molecules such as Mn_{12} clusters), so that they become oxidized by adsorbed water and atmospheric adventitious trace O_2 (during or after reaction) (S5, Supplementary Information). This observation might explain why the O 1s XPS ratio is somewhat greater than expected, 3:1, from 32 oxygen atoms in methacrylate molecules, 4 oxygen atoms from H_2O molecules (532.5 eV), 12 oxygen atoms from the $Mn_{12}O_{12}$ core (530 eV). The C region exhibits four components, shown on deconvolution of the principal C 1s line (285 eV) 285.2 eV, (C–Si) 292.9 eV, (O–C=O) 286.9 eV and 288.7 eV (aliphatic backbone) [24] (S6, Supplementary Information).

If the Mn_{12}–(methacrylate) clusters were all spatially oriented with the Mn_{12} core parallel to the surface through the JT axis, one would expect a correlation between the orientation of Mn_{12}–(methacrylate)–Si(100) through the Si 2p and Mn 2p XPS data. This correlation is obtainable with simple calculations and the following structural parameters: a) Si(100) lattice parameter a = 5.42 Å and Mn_{12}–(methacrylate) cluster diameter about 16.93 Å; b) on assuming an entirely Si(100) surface as tightly packed implying binding of only one carbon atom to the Si(100) surface, exclusion of overlap between molecules, and area ratios of maximum extent for each molecule. The resulting monolayer area ratio of covered to not covered is about 0.64, so that each Mn_{12}–(methacrylate) cluster blocks 24 Si sites.ç

Electrochemical measurements

The CV plot of Mn_{12}–(methacrylate) in acetonitrile has several cathodic and anodic waves matching those reported for $[Mn_{12}O_{12}(O_2CR)_{16}(H_2O)_4]$, (R = Me, Et, Ph) (Figure 4).

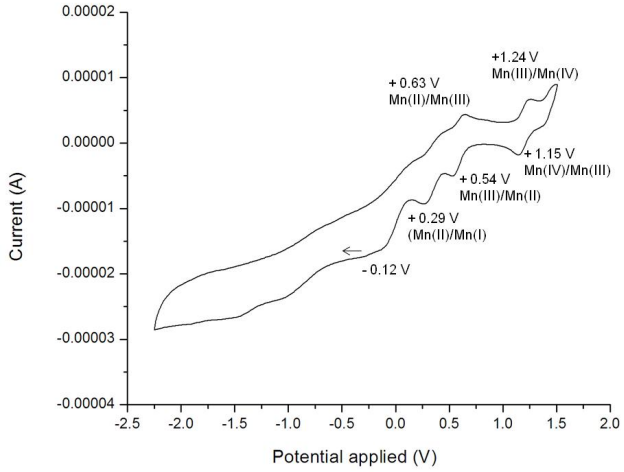

FIGURE 4. Cyclic voltammogram of Mn_{12}–(methacrylate) using Ag/AgCl as reference electrode in NBu_4ClO_4 (0.25 mol L^{-1}) in acetonitrile, scan rate 0.100 V s^{-1}.

The following reactions summarize the electron transfers proposed to occur in solution at the $Mn_{12}O_{12}$ core [25, 26] **(1).**

$$[Mn_{12}O_{12}]^{+} \rightleftharpoons [Mn_{12}O_{12}] \rightleftharpoons [Mn_{12}O_{12}]^{-} \rightarrow [Mn_{12}O_{12}]^{2-} \rightarrow [Mn_{12}O_{12}]^{3-} \quad (1)$$

The transformations involving oxidation and three subsequent reductions are likely centred at the outer Mn(III) and cubane Mn(IV) ions, respectively. The thermodynamic preference for reduction of Mn(III) to Mn(II) over Mn(IV) to Mn(III) indicates that the latter process leaves unaffected the cubane Mn(IV), as it is inhibited because of the large reorganization energy. As the Mn(IV) ions are each bound to five hard O^{2-} ions, they favor higher oxidation states, which disfavor reduction to Mn(III). If the reduction to Mn(III) ion occurred, it would generate a JT distortion causing strain in the rigid Mn(IV) cubane. Conversely, little perturbation of the $Mn_{12}O_{12}$ core on reduction of an outer Mn(III) ion is observed [14]. To acquire an understanding of the reactivity of the functionalized silicon surfaces, we initially tested a cell (S2, Supplementary Information) with dropping CH_2Cl_2 (electric permittivity, ε_o = 8.93), acetonitrile (MeCN, electric permittivity, ε_o = 37.5) and tetrahydrofuran (THF, electric permittivity, ε_o = 7.58), but the drop required to effect a contact between the working electrode (surface as prepared) and the Ag counter/reference electrode failed to form, likely because of the similar chemical affinities of these solvents with the surface nature upon functionalization. Additionally, CH_2Cl_2 and MeCN readily evaporate during measurement with the working electrode. With THF as solvent, the functionalization decomposes to native Si oxide, shown by XPS survey signals of oxygen atoms (S7, Supplementary Information). In contrast, in an aqueous medium both the shape and stability of the drop (H_2O electric permittivity, ε_o = 80.1) significantly improved the electrochemical experiments. The CV of Mn_{12}–(methacrylate)–Si(100) has two cathodic signals at –0.76 and –0.44 V, with no matching oxidative signals, indicating chemical irreversibility (Figure 5). These signals are tentatively assigned to processes Mn(IV)/Mn(III) and Mn(III)/Mn(II) [25, 26]. The calculated charge at –0.44 V is 3.14 x 10^{-5} C cm^{-2}.

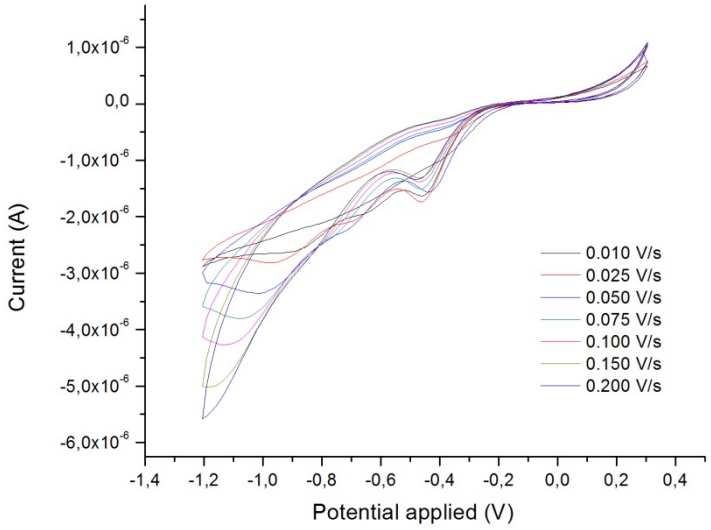

FIGURE 5. Cyclic voltammograms of Mn_{12}–methacrylate–Si(100) with a piece of *n*–type Si semiconductor as working electrode in KCl (3 mol L^{-1}) at varied rates of potential scan.

Although CV measurements were implemented in water that might be counterproductive because of prospective corrosion of the surface, Mn_{12}–(methacrylate)–Si(100) underwent no apparent surface decomposition, as demonstrated with varied scan rates, indicating robustness of Si–C and the metal core (Figure 5). Furthermore, blank experiments performed with non–hydrogen– and hydrogen–terminated Si(100) electrodes under similar conditions of measurement used for Mn_{12}–(methacrylate)–Si(100) (S8, Supplementary Information) were devoid of cathodic or anodic waves over the entire potential sweep.

Electrochemical impedance is generally measured on applying a sinusoidal AC perturbation of potential over the applied base potential. This perturbation involves a wide frequency range to probe the various elements and their time coefficients in an investigated system [27, 28, 17, 29]. EIS of Mn_{12}–(methacrylate)–Si(100) were performed with AC modulation and frequency range 20 kHz to 0.100 Hz. The Nyquist plots (Figure 5) were fitted to an equivalent circuit model used by Creager et al. [30]. Using ideal elements in the equivalent circuits for electrochemical systems presents difficulties in processing the data because of the non–linearity of real systems; for that reason, constant–phase elements (CPE) are used in proposed equivalent circuits [27]. The equivalent-circuit model includes a series resistance (resistance of both the electrolyte solution and the series resistance from cables and contacts, R_{SOL}), the double–layer capacitance (Helmholtz capacitance, C_{DL}), and charge transfer or polarization resistance (R_{CT}), and adsorption pseudocapacitance (C_{AD}). The double–layer capacitance is in parallel with the charge-transfer resistance (Inset, Figure 6). R_{SOL} comprises the resistance between the reference electrode and the Mn_{12}–modified silicon electrode and the resistance arising from cables and contacts. Importantly, to minimize the variation of R_{SOL} for every measurement, the position of the two electrodes and the distance between the two electrodes were maintained constant; the preliminary results are listed in Table 2. The Nyquist plot for Mn_{12}–(methacrylate)–Si(100) is a semicircle of which the value on the real axis (in–phase impedance) at the high-frequency intercept yields R_{SOL} (24.9 Ω). The value on the real axis at the other (low-frequency) intercept is the sum of the polarization resistance and the solution resistance; the diameter of the semicircle is hence equal to the polarization resistance (348 kΩ), and for hydrogen–modified Si is 150 kΩ. R_{CT} is larger for

Mn_{12}–modified than for H–Si(100) because the film thickness increased upon Mn_{12} tailoring, which has a large reorganization energy and a sluggish electron transfer (Figure 6). For non-hydrogen-terminated Si, the insulating native oxide causes electron transfer to be slow, which produces an electrical resistivity several orders of magnitude greater than for functionalized Si. The capacitive double–layer (660 nF) of Mn_{12}–(methacrylate)–Si(100) is larger than of H–terminated Si (129 pF) (S9, Supplementary Information). To calculate the electron–transfer rate coefficient of Mn_{12}–(methacrylate)–Si(100) we used the following equations (**2–5**) [30, 31],

$$C_{DL} = (C/A)\,A \tag{2}$$

$$C_{AD} = {(F^2 A\Gamma)}\Big/{(4RT)} \tag{3}$$

$$R_{CT} = {(2RT)}\Big/{(F^2 A\Gamma k_{et})} \tag{4}$$

in which C_{DL} denotes the double–layer capacitance, C/A is the double–layer capacitance per unit area, A is the electrode area, Γ is the coverage of electroactive species per unit area, C_{AD} is the adsorption pseudocapacitance, R_{CT} is the charge–transfer resistance; the remaining quantities have their conventional significance. The rate coefficient for electron transfer is obtained with equation (**5**).

$$k_{ET} = \frac{1}{(2\,R_{CT}\,C_{AD})} \tag{5}$$

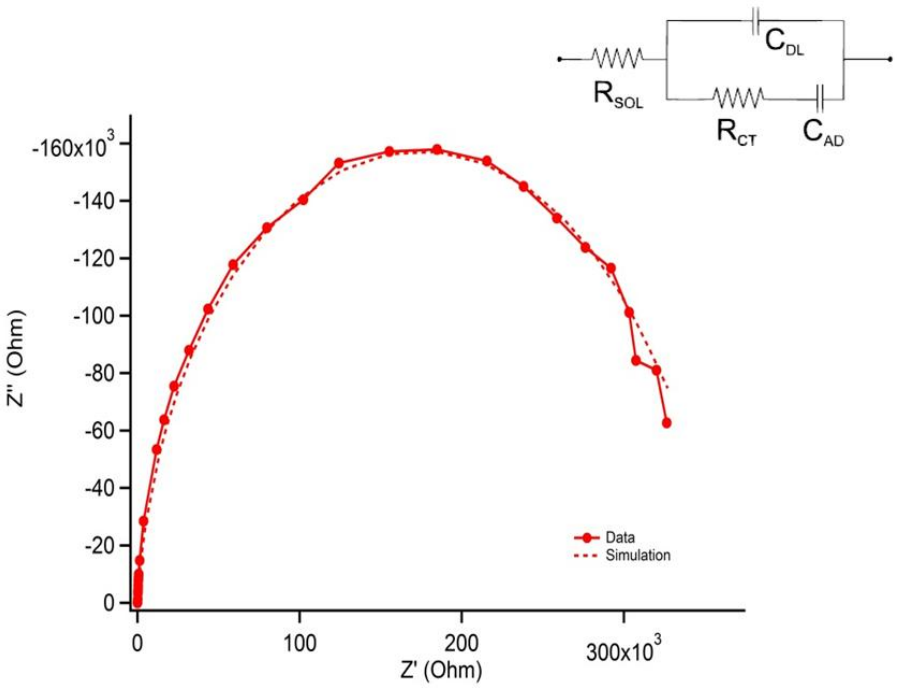

Figure 5. Nyquist plot of Mn_{12}–(methacrylate)–Si(100). The red circle (solid line) represents experimental data; the dotted lines correspond to the fit. The inset shows the equivalent circuit model.

k_{ET} (2.6 x 10^{-2} s^{-1}) for Mn_{12}–(methacrylate)–Si(100) indicates a slow electron transfer, which might be attributed to electronic and structural limiting factors. In related systems, the rates of electron transfer in ferrocene–containing alkanethiolate monolayers on gold electrodes are about 9 –13 s^{-1}, and for zinc(II) porphyrins over Si on the order of 10^4 s^{-1} [30, 29].

Table 2. Best fitted equivalent-circuit parameters to impedance data in the complex plane at the potential maximum for Mn_{12}–(methacrylate)–Si(100).

R_{sol} / Ω	C_{DL} / nF	R_{CT} / kΩ	C_{AD} / μF	k_{ET} / s^{-1}
24.9	660	348	55	0.026

IV. CONCLUSION

We demonstrate the facile and direct chemisorption of Mn_{12}–(methacrylate) onto H–Si(100) through covalent Si–C bonds to form Mn_{12}–(methacrylate)–Si(100) as described with AFM, XPS and electrochemical data. Mn_{12}–(methacrylate)–Si(100) is electrochemically active, highlighting the advantages of transition elements on a surface. CV and EIS findings indicate that Mn_{12}–(methacrylate) on a surface has inherent electronic and structural features that cause slow electron transfer. Future work in this area will focus on anchoring clusters of less nuclearity and varied core geometry such as Mn_6.

V. REFERENCES

[1] Asanuma, H.; Bishop, E. M.; Yu, H. Z., *Electrochem. Acta*. **2007**, 52, 2913–2919.

[2] Lindford, M. R.; Fenter, P.; Eisenberg, P. M.; Chidsey, C. E. D., *J. Am. Chem. Soc.* **1995**, 117, 3145 –3155.

[3] Motta, A.; Condorelli, G. G.; Pellegrino, G.; Cornia, A.; Fragalà, I. L., *J. Phys. Chem. C*. **2010**, 114, 20696–20701.

[4] Cornia, A.; Fabretti, A. C.; Pacchioni, M.; Zobbi, L.; Bonacchi, D.; Caneshi, A.; Gatteschi, D.; Biagi, R.; Del Pennino, U.; De Renzi, V.; Gurevich, L.; Van der Zant, H. S. J., *Angew. Chem. Int. Ed.* **2003**, 42, 1645–1648.

[5] Zobbi, L.; Manninni, M.; Pacchioni, M.; Chastanet, G.; Bonacchi, D.; Zanardi, C.; Biagi, R.; Del Pennino, U.; Gatteschi, D.; Cornia, A.; Sessoli, R., *Chem. Commun*. **2005**, 1640–1642.

[6] Rappich, J.; Merson, A.; Roodenko, K.; Dittrich, T.; Gensch, M.; Hinrichs, K.; Shapira, Y. *J., Phys. Chem. B.* **2006**, 110, 1332–1337.

[7] Boukherroub, R. D.; Wayner, D. M., *J. Am. Chem. Soc.* **1999**, 121, 11513–11515.

[8] Rohde, R. D.; Agnew, H. D.; Yeo, W. S.; Bailey, R. C.; Heath, J. R. *J. Am. Chem. Soc*. **2006**, *128*, 9518–9525.

[9] Sun, Q. Y.; de Smet, L. C. P. M.; van Lagen, B.; Giesbers, M.; Thüne, P. C.; van Engelenburg, J.; de Wolf, F. A.; Zuilhof, H.; Sudhölter, E. J. R. *J., Am. Chem. Soc*. **2005**, 127, 2514–2523.

[10] Sieval, A. B.; van den Hout, B.; Zuilhof, H.; Sudhölter, E. J. R., *Langmiur*. **2001**, 17, 2172–2181.

[11] Ng, A.; Ciampi, S.; James, M.; Harper, J. B.; Gooding, J. J., *Langmiur*. **2009**, 25, 13934–13941.

[12] Condorelli, G. G.; Motta, A.; Fragalà, I. L.; Giannazzo, F.; Raineri, V.; Caneshi, A., Gatteschi, D. *Angew. Chem. Int. Ed.*, **2004**, 43, 4081–4084.
[13] Fleury, B.; Catala, L.; Huc, V.; David, C.; Zhong, W. Z.; Jegou, P.; Baraton, L.; Palacin, S.; Albouy, P. A.; Mallah, T., *Chem. Commun*. **2005**, 2020–2022.
[14] Condorelli, G. G., Motta, A. ; Favazza, M. ; Nativo, P. ; Fragalà, I. L. ; Gatteschi, D., *Chem. Eur. J.* **2006**, 12, 3558–3566.
[15] Bagai, R.; Christou, G., *Chem. Soc. Rev.* **2009**, 38, 1011-1026.
[16] Sánchez, A.; Urcuyo, R.; Gónzalez-Flores, D.; Montalberth-Smith, R.; León-Rojas, C.; Pineda, L. W.; Montero, M. L., *Surf. Sci*. **2012**, 606, 527–535.
[17] Cummings, S. P.; Savchenko, J.; Ren, T., *Coord. Chem. Rev*. **2011,** 255, 1587–1602.
[18] Willemin, S.; Donnadieu, B.; Lecren, L.; Henner, B.; Clérac, R.; Guérin, C.; Meyer, A.; Pokrovskii, A. V.; Larinova, J., *New. J. Chem*. **2004,** 28, 919–928.
[19] Roth, K. M.; Yasseri, A. A.; Liu, Z.; Dabke, R. B.; Malinovskii, V.; Schweikart, K. H.; Yu, L.; Tiznado, H.; Zaera, F.; Lindsey, J. S.; Kuhr, W. G.; Bocian, D. F., *J. Am. Chem. Soc*. **2003,** 125, 505–517.
[20] Aswal, D.K.; Lenfant, S.; Guerin, D.; Yakhmi, J. V. ; Vuillaume, D., *Anal. Chim. Acta.* **2006**, 568, 84–108.
[21] Boukherroub, R.; Morin, S.; Bensebaa, F.; Wayner, D. D. M., *Langmiur.* **1999,** 153, 831–3835.
[22] Lis, T., *Acta Cryst. B36*. **1980**, 2042–2046.
[23] Ribas Gispert, J., *Coordination Chemistry*, ed. Wiley-VCH: Weinheim Germany, 2008, pp 81–90
[24] Otero, G.; Evangelio, E., Rogero, C.; Vásquez, L.; Gómez–Segura, J.; Martín Gago, J. A. M.; Ruiz–Molina, D., *Langmiur*. **2009**, 25, 10107–10115.
[25] Sessoli, R., Tsai, H–L.; Schake, A. R.; Wang, S.; Vincent, J. B.; Folting, K.; Gatteschi, D.; Christou, G.; Hendrickson, D. N., *J. Am. Chem. Soc*. **1993**, 115, 1804–1816.
[26] Eppley, H. J.; Tsai, H–L.; de Vries, N.; Folting, K. D.; Christou, G.; Hendrickson, D. N., *J. Am. Chem. Soc*. **1995**, 117, 301–317.
[27] Scholz, F. (Ed.), *Electroanalytical Methods: Guide to Experiments and Applications*, ed. Springer: Berlin Germany , 2nd ed., 2010, pp 159–177.
[28] Hamman, C. H.; Hamnett, A.; Vielstich, W., *Electrochemistry*, ed. Wiley-VCH: Weinheim Germany, 2nd ed., 2007, pp 278–291.
[29] Kissinger, P. T.; Heineman, W. R., *J. Chem. Ed.* **1983**, 60, 702–706.
[30] Creager, S. E.; Wooster, T. T., *Anal. Chem*. **1998**, 70, 4257–4263.
[31] Conway, B. E.; Birss, V.; Wojtowicz, J., *J. Power Sources*. **1997**, 66, 1–14.

ACKNOWLEDGEMENTS

Project Nº 115–B1–168 from the Vicerrectoría de Investigación, Centro de Electroquímica y Energía Química (CELEQ), and Escuela de Química, Universidad de Costa Rica provided support of this work.

We thank M.Sc. Alejandra Sánchez and Dr. Sergio A. Paniagua at Georgia Institute of Technology, USA, for recording XPS, Dr. Daniel Azofeifa (CICIMA) and M.Sc. Roberto Urcuyo (CELEQ) for fruitful discussion.

SUPLEMENTARY INFORMATION

Drawing of Mn_{12}–OAc structure, electrochemical cell setup, AFM image of hydrogen–terminated silicon, survey XPS of Mn_{12}–modified silicon, high-resolution XPS of O 1s, C 1s and O 1s regions (reaction in THF) in Mn_{12}–(methacrylate)–Si(100), cyclic voltammogram of non-hydrogen terminated *n*–type Si(100) electrode, and Nyquist plots of passivated H–Si(100) electrode are available in the Supplementary Information.